Propofol improves neuronal apoptosis and oxidative damage mediated by cerebral ischemia-reperfusion by regulating the miR-6838-5p/AQP11 axis

Keywords
miRNA, Stroke, Cerebral infarction, Middle cerebral artery occlusion/reperfusion, Anesthetic

Abstract

Introduction

This study aimed to elucidate the mechanism by which Propofol (PPF) exerts its effects in cerebral ischemia-reperfusion injury (CI/RI).

Material and methods

A rat model of CI/RI was established via middle cerebral artery occlusion/reperfusion (MCAO/R). MCAO/R rats were pre-treated with PPF (10 mg/kg) via intraperitoneal injection. Additionally, 48 hours before PPF administration, miR-6838-5p agomir/antagomir and aquaporin-11 (AQP11) lentiviral overexpression vectors were injected into MCAO/R rats. Infarct size was determined using 2,3,5-triphenyl tetrazolium chloride staining. Neurological function was assessed using standardized scoring, and cerebral edema was measured by determining brain water content. Hematoxylin-eosin staining, Nissl staining, and Terminal deoxynucleotidyl transferase dUTP nick end labeling staining were performed on brain tissues. Inflammatory and oxidative markers were evaluated. A hypoxia/reoxygenation (H/R) injury model was established in PC12 cells to assess miR-6838-5p and AQP11 expression levels, as well as cell viability and apoptosis.

Results

The lethal dose 50 (LD□□) of PPF in rats was determined to be 22.6 mg/kg, significantly higher than the therapeutic dose. PPF or overexpression of miR-6838-5p resulted in reduced cerebral infarct size, neuronal necrosis, and apoptosis, increased Nissl bodies, and decreased brain edema, apoptosis, tumor necrosis factor-α, interleukin-1β, and malondialdehyde (MDA) levels. Glutathione peroxidase (GSH-Px) and superoxide dismutase (SOD) activities were elevated in MCAO/R rats treated with PPF. These protective effects of PPF were reversed by miR-6838-5p knockdown or AQP11 overexpression. PPF ameliorated H/R-induced neuronal damage, enhanced neuronal activity, reduced apoptosis and MDA production, and increased GSH-Px and SOD levels.

Conclusions

PPF ameliorates CI/RI by modulating the miR-6838-5p/AQP11 axis.

Preprint

Propofol improves neuronal apoptosis and oxidative damage mediated by cerebral ischemia-reperfusion by regulating the miR-6838-5p/AQP11 axis

Short title: Propofol in cerebral ischemia-reperfusion

Abstract

Objective: This study aimed to elucidate the mechanism by which Propofol (PPF) exerts its effects in cerebral ischemia-reperfusion injury (CI/RI).

Materials and Methods: A rat model of CI/RI was established via middle cerebral artery occlusion/reperfusion (MCAO/R). MCAO/R rats were pre-treated with PPF (10 mg/kg) via intraperitoneal injection. Additionally, 48 hours before PPF administration, miR-6838-5p agomir/antagomir and aquaporin-11 (AQP11) lentiviral overexpression vectors were injected into MCAO/R rats. Infarct size was determined using 2,3,5-triphenyl tetrazolium chloride staining. Neurological function was assessed using standardized scoring, and cerebral edema was measured by determining brain water content. Hematoxylin-eosin staining, Nissl staining, and Terminal deoxynucleotidyl transferase dUTP nick end labeling staining were performed on brain tissues. Inflammatory and oxidative markers were evaluated. A hypoxia/reoxygenation (H/R) injury model was established in PC12 cells to assess miR-6838-5p and AQP11 expression levels, as well as cell viability and apoptosis.

Results: The lethal dose 50 (LD_{50}) of PPF in rats was determined to be 22.6 mg/kg, significantly higher than the therapeutic dose. PPF or overexpression of miR-6838-5p resulted in reduced cerebral infarct size, neuronal necrosis, and apoptosis, increased Nissl bodies, and decreased brain edema, apoptosis, tumor necrosis factor-α, interleukin-1β, and malondialdehyde (MDA) levels. Glutathione peroxidase (GSH-Px) and superoxide dismutase (SOD) activities were elevated in MCAO/R rats treated with PPF. These protective effects of PPF were reversed by miR-6838-5p knockdown or AQP11 overexpression. PPF ameliorated H/R-induced neuronal damage, enhanced neuronal activity, reduced apoptosis and MDA production, and increased GSH-Px and SOD levels.

Conclusion: PPF ameliorates CI/RI by modulating the miR-6838-5p/AQP11 axis.

Keywords: Middle cerebral artery occlusion/reperfusion; Anesthetic; miRNA; Stroke; Cerebral infarction

Introduction

Ischemic stroke is a major cause of morbidity and mortality, leading to a range of complications such as cognitive impairment and epilepsy [1, 2]. With its increasing prevalence worldwide, ischemic stroke represents a significant public health burden, contributing to long-term disability and reduced quality of life among survivors [3]. Cerebral ischemia-reperfusion injury (CI/RI) occurs when blood supply returns to ischemic brain tissue, typically during the treatment of ischemic stroke [4, 5]. CI/RI involves multiple pathophysiological mechanisms, including inflammation, oxidative stress, accumulation of metabolic toxins, and apoptosis, which collectively exacerbate brain injury [6, 7]. Current therapeutic strategies, which mainly aim to restore blood flow via thrombolysis or mechanical thrombectomy, are often limited by narrow therapeutic windows and the risk of adverse effects, highlighting the urgent need for adjunctive treatments that can mitigate the damaging consequences of reperfusion [8]. Despite extensive research, effective treatments for CI/RI remain elusive, making the exploration of its pathogenesis and the development of therapeutic interventions critical [9].

Propofol (PPF), a 2,6-diisopropylphenol-based intravenous general anesthetic, is widely used for anesthesia and sedation. Beyond its anesthetic properties, PPF shows multiple pharmacological effects, which encompass antioxidant, anti-inflammatory, and neuroprotective functions [10, 11], which make it a promising candidate for therapeutic intervention in CI/RI. Beyond its anesthetic properties, PPF possesses antioxidant, anti-inflammatory, and neuroprotective effects [12, 13]. Increasing preclinical evidence indicates that PPF

Preprint

offers pharmacological benefits in various diseases, including cardiovascular and cerebrovascular disorders [14-16], cancer [17], and neurodegenerative diseases [18, 19]. Notably, several studies have demonstrated that PPF pretreatment can mitigate CI/RI-induced brain damage by attenuating oxidative stress and apoptosis [20-23]. Nonetheless, the specific molecular processes responsible for these protective effects are not well comprehended. Recent research has revealed that PPF may exert its neuroprotective effects through epigenetic regulation, particularly by altering the expression patterns of microRNAs (miRNAs), which are crucial post-transcriptional regulators during ischemic injury. For instance, miR-6838-5p was reported to be downregulated in CI/RI and to protect the blood–brain barrier by targeting PDCD4 [24]. However, whether miR-6838-5p also affects CI/RI by regulating other downstream mRNAs remains to be further elucidated. Notably, AQP11, a member of the aquaporins (AQPs) family, is a transmembrane protein that transports water and small solutes [25]. AQP11 has been found to be abundantly expressed in brain tissues but its role and function in brain tissues are unknown [26]. Based on previous bioinformatics analysis, we identified a potential binding site for miR-6838-5p and AQP11. Therefore, we hypothesized that miR-6838-5p might be involved in the CI/RI process by targeting AQP11.

This investigation sought to determine the effects of PPF on CI/RI and to explain its molecular mechanisms by employing a middle cerebral artery occlusion/reperfusion (MCAO/R) rat model and a hypoxia/reoxygenation (H/R) injury model in PC12 cells. Specifically, we focused on the role of the miR-6838-5p/AQP11 axis as a novel research target, potentially contributing to the neuroprotective effects of PPF in CI/RI.

Materials and Methods

Laboratory Animals

A total of 240 specific pathogen-free male Sprague-Dawley (SD) rats (8-10 weeks old, 250 ± 30 g) were obtained from Jinan Pengyue Animal Breeding Co., Ltd. The rats were kept under specific conditions (23 ± 2°C, 55 ± 5% humidity) with a 12-hour light/dark cycle and had unrestricted access to food and water. In order to minimize experimental bias and ensure the scientific validity and reliability of the results, all rats were assigned to different experimental groups or control groups according to the needs of the study by third-party staff unrelated to the subsequent operations using the random number table method prior to the experiment. At the same time, in order to prevent subjective interference and information bias, the experimental operators and data collectors were kept in ignorance of the information on grouping until after all operations and data recording had been completed, and then the grouping was blinded and statistically analyzed by a third-party. All animal experiments were conducted in accordance with the National Institutes of Health (NIH) guidelines and were approved by the Animal Care and Use Committee of our Hospital (Approval Number: SDTHEC).

Rat MCAO/R Model

A MCAO/R rat model was established using a surgical procedure as previously described [27]. Briefly, rats were anesthetized via intraperitoneal injection of 3% (w/v) pentobarbital sodium (40 mg/kg). The left internal carotid artery was exposed, and a 4/0 surgical nylon monofilament was inserted to occlude blood flow in the middle cerebral artery, internal carotid artery, anterior cerebral artery, and posterior cerebral artery. After 2 hours of occlusion, the filament was withdrawn to allow reperfusion for 24 hours. Body temperature was maintained at approximately 37°C throughout the procedure. No instances of peritonitis or intestinal obstruction were observed post-anesthesia. Rats in the sham group underwent the same surgical procedure without filament insertion.

Rat Treatments

SD rats were randomly assigned to six groups (n = 6 per group), with PPF dosing adjusted based on body weight [28]:

Sham Group (As a negative control for the MCAO/R group): rats underwent sham surgery and received

Preprint

an intraperitoneal injection of normal saline 10 minutes prior to surgery.

MCAO/R Group: rats underwent MCAO/R and received an intraperitoneal injection of normal saline 10 minutes prior to surgery.

MCAO/R + Dimethyl Sulfoxide (DMSO) Group (as a negative control for the MCAO/R + PPF group): rats underwent MCAO/R and received an intraperitoneal injection of 0.01% DMSO 10 minutes prior to surgery.

MCAO/R + PPF Group: rats underwent MCAO/R and received an intraperitoneal injection of PPF (10 mg/kg; Xiyuan-Bio, Shanghai, China) 10 minutes prior to surgery [29, 30]. The chemical structure of PPF is illustrated in Fig. 1A.

MCAO/R + agomiR-NC Group: After anesthesia, rats were injected with agomiR-NC prior to MCAO/R.

MCAO/R + agomiR-miR-6838-5p Group: After anesthesia, rats were injected with agomiR-miR-6838-5p prior to MCAO/R.

Additional groups included combinations of PPF with antagomirs and lentiviral vectors:

MCAO/R + PPF + anta-NC Group: After anesthesia, rats were injected with antagomir-NC. After 48 hours, rats received an intraperitoneal injection of PPF (10 mg/kg) and underwent MCAO/R.

MCAO/R + PPF + anta-miR-6838-5p Group: After anesthesia, rats were injected with antagomir-miR-6838-5p. After 48 hours, rats received an intraperitoneal injection of PPF (10 mg/kg) and underwent MCAO/R.

MCAO/R + PPF + LV-NC Group: After anesthesia, rats were injected with antagomir-miR-6838-5p and LV-NC. After 48 hours, rats received an intraperitoneal injection of PPF (10 mg/kg) and underwent MCAO/R.

MCAO/R + PPF + LV-AQP11 Group: After anesthesia, rats were injected with antagomir-miR-6838-5p and LV-AQP11. After 48 hours, rats received an intraperitoneal injection of PPF (10 mg/kg) and underwent MCAO/R.

Using a microsyringe, 50 μL of lentivirus was slowly injected into the right cerebral cortex of the rats. AgomiR-NC, agomiR-miR-6838-5p, lentiviral vectors for AQP11 (LV-AQP11), and non-targeting plasmid (LV-NC) were obtained from RIBOBIO (Guangzhou, China). From a total of 65 rats, 59 were treated with MCAO/R, and 6 had sham operations. The study excluded five rats that died during the MCAO/R treatment and intraperitoneal injection. No mortality was observed in the sham group. Following the modeling, rats were put down by cervical dislocation, and brain tissues were extracted.

Neurological Deficit Score

At 24 hours post-reperfusion, neurological deficits were evaluated using a standardized scoring system: 0 = no deficit; 1 = failure to fully extend the contralateral forepaw; 2 = incomplete forepaw extension; 3 = mild contralateral rotation; 4 = vigorous contralateral rotation; 5 = falling to the contralateral side. All assessments were conducted by a blinded investigator [31].

Measurement of Brain Edema

The measurement of cerebral edema was conducted by assessing the water content in the brain. To determine the wet weight (WW), the cerebral hemispheres underwent weighing, followed by a drying process at 105°C over 24 hours to ascertain the dry weight (DW). The formula for determining brain water content was: Brain water content = (WW - DW)/WW × 100% [32].

2,3,5-Triphenyl Tetrazolium Chloride (TTC) Staining

Brain tissues were incubated on ice for 24 hours, sectioned into continuous coronal slices, and placed in 2% TTC staining solution at 37°C for 20 minutes. TTC staining was halted by washing with phosphate-buffered saline (PBS), and tissues were fixed in 4% paraformaldehyde for 2 hours. Infarcted regions appeared unstained and were quantified as infarct volume relative to total brain volume using Image Pro Plus 6.0 software. The formula for infarct volume is the total infarct volume divided by the total brain volume, then multiplied by 100%.

Hematoxylin and Eosin (HE) Staining

Rat brain tissues were fixed in 4% paraformaldehyde (Sigma-Aldrich, Merck KGaA), subsequently

Preprint

hydrated and permeabilized. Tissues were then embedded in paraffin, sectioned into 4 μm slices, and subjected to HE staining. Each slice was examined under a light microscope at 200× magnification in three fields.

Nissl Staining

Paraffin-embedded brain sections were dehydrated and stained with cresyl violet solution for 1 hour. Following staining, slices were rinsed sequentially with 70%, 80%, and 95% ethanol (10 seconds each), dehydrated with anhydrous ethanol (5 minutes per step, twice), cleared with xylene (5 minutes each step, twice), mounted with neutral gum, and observed under a microscope (Nikon).

Terminal deoxynucleotidyl Transferase dUTP Nick End Labeling (TUNEL) Staining

The TUNEL staining process utilized a TUNEL kit (Qiming Bio Engineering Co., Ltd., Shanghai, China; OX02752). Sections of rat brain tissue underwent fixation using 4% paraformaldehyde for 20 minutes, were made permeable using 0.1% TritonTM X-100 for 5 minutes, and then subjected to incubation with a TUNEL reaction blend (in darkness at 37°C for one and a half hours). The samples underwent counterstaining using 4,6-diamidino-2-phenylindole (DAPI). Apoptotic cells testing positive for TUNEL were measured through fluorescence microscopy [33].

Enzyme-Linked Immunosorbent Assay (ELISA)

Rat brain tissues were homogenized in PBS on ice and centrifuged at 3500 rpm for 15 minutes. The supernatant was collected, and levels of tumor necrosis factor-α (TNF-α; orb79138, Biorbyt) and interleukin-1β (IL-1β; orb79117, Biorbyt) were measured using respective ELISA kits. Absorbance was read at 450 nm using a microplate reader (RT-6100, LeiDu).

Determination of Oxidative Stress Indicators

Malondialdehyde (MDA), glutathione peroxidase (GSH-Px), and superoxide dismutase (SOD) in rat brain tissues and PC12 cells were quantified using specific detection kits (JK-(a)-2197, JK-(a)-2396, JK-(a)-2293; Jingkang Bioengineering Co., Ltd., Shanghai, China).

Cell Culture

PC12 cells, sourced from the China Center for Type Culture Collection in Wuhan, China, were grown in Dulbecco's Modified Eagle Medium (DMEM), enriched with 10% fetal bovine serum (Beyotime, Shanghai, China), 100 U/mL penicillin, and 0.1 mg/mL streptomycin (Invitrogen), in an environment at 37°C and 5% CO2. For the creation of the H/R injury model, PC12 cells were categorized into three distinct groups:

Control Group: Growing in a normoxic environment (21% O_2, 5% CO_2, 74% N_2) devoid of PPF treatment.

Group H/R: subjected to hypoxia (1% O_2, 5% CO_2, 94% N_2) for two hours, then reoxygenated in normoxic environments.

H/R + PPF Group: Pre-treated with PPF (50 μM; Sigma-Aldrich) for 1 hour prior to H/R injury [34].

Cell Viability

PC12 cells (2×10^3 cells/well) were seeded into 96-well plates and incubated at 37°C in 5% CO_2 for 72 hours. Cell viability was assessed using the 3-(4,5-dimethyl-2-thiazolyl)-2,5-diphenyl-2-H-tetrazolium bromide (MTT) assay kit (Sigma-Aldrich). Briefly, 20 μL of MTT solution was added to each well and incubated at 37°C for 4 hours. Subsequently, 150 μL of dimethyl sulfoxide (DMSO; Sigma-Aldrich) was added to dissolve the formazan crystals. Optical density was measured at 570 nm using a Bio-Tek microplate reader (Hopkinton, MA, USA).

Cell Apoptosis

The measurement of apoptosis was conducted with the Annexin V-fluorescein isothiocyanate (FITC)/propidium iodide (PI) Apoptosis Detection Kit (Sangon Biotech, Shanghai, China). PC12 cells, totaling 5×10^5 cells per well, were cultured in 6-well plates and subjected to a 5-minute incubation with 5 μL Annexin V-FITC and 10 μL PI at ambient temperature in darkness. The analysis of flow cytometry utilized a FACS Verse flow cytometer (BD Biosciences), and the data underwent examination through FlowJo software (version 10; TreeStar) [35].

Preprint

Quantitative Analysis of mRNA Expression

RNA was extracted from brain tissues and PC12 cells using Trizol reagent (Invitrogen). For miRNA analysis, cDNA was synthesized using the TaqMan MicroRNA Reverse Transcription Kit (Applied Biosystems) with specific stem-loop RT primers. For mRNA analysis, cDNA was synthesized using the PrimeScript RT kit (Takara). Expression levels of miR-6838-5p and AQP11 were quantified using SYBR Green Real-Time PCR Master Mix (Takara) on a 7500 Real-Time PCR System (Applied Biosystems). The internal control for AQP11 was β-actin, and miR-6838-5p was referenced using U6. Primer sequences are listed in Table 1.

Quantitative Analysis of Protein Expression

Proteins were harvested from rat brain mixtures utilizing the radioimmunoprecipitation assay lysis buffer (Beyotime). Protein concentrations were ascertained through the application of a bicinchoninic acid protein assay kit. The proteins underwent denaturation through boiling, were separated using sodium dodecyl sulfate-polyacrylamide gel electrophoresis , and then moved onto a polyvinylidene fluoride membrane, which was blocked using 5% skim milk and subjected to an overnight incubation at 4°C with primary antibodies targeting AQP11 (1:100; ab122821, Abcam), AQP1 (1:1000; AB2219, MilliporeSigma), AQP4 (1:1000; AB3594, MilliporeSigma), AQP9 (1:1000; sc-74409, Santa Cruz Biotechnology), and β-actin (1:1000; ab8277, Abcam). The membrane underwent incubation with a horseradish peroxidase-labeled goat anti-rabbit IgG secondary antibody (1:10,000; AB175781, Abcam) at ambient temperature for an hour. The visualization of protein bands was achieved through the use of an enhanced chemiluminescence agent. The intensities of the bands were measured utilizing the ImagePro Plus 6.0 software.

Luciferase Reporter Gene Assay

TargetScan software predicted that miR-6838-5p targets AQP11. Wild-type (AQP11-WT) and mutant (AQP11-MUT) fragments containing potential miR-6838-5p binding sites were cloned into the pMIR-REPORT plasmid vector (Promega). The luciferase reporter constructs were co-transfected with miR-6838-5p mimic into PC12 cells using Lipofectamine 2000 reagent (Invitrogen). After 24 hours, luciferase activity was measured using a luciferase assay kit (Promega) [36].

RNA Immunoprecipitation (RIP) Assay

RIP assays were conducted using a RIP kit (Millipore). Cells were lysed with RIP lysis buffer, and the lysate was incubated with RIP buffer containing human anti-AGO2-conjugated magnetic beads. The immunoprecipitated complexes were treated with protease K to digest proteins, and the associated RNA was isolated. The presence of miR-6838-5p and AQP11 in the precipitated RNA was determined by RT-qPCR [37].

Statistical Analysis

Data were analyzed using SPSS version 21.0 software. Normality was assessed using the Kolmogorov-Smirnov test. Results are presented as mean ± standard deviation. For comparisons involving multiple groups, one-way analysis of variance followed by the least significant difference post hoc test was used. Categorical data (rates or percentages) were compared using the chi-square test. All statistical analyses were two-tailed, with a p-value under 0.05 deemed statistically significant.

Results

PPF Mitigates Oxidative Stress Injury in MCAO/R Rats

To investigate the role of PPF in CI/RI, a MCAO/R rat model was established, and PPF treatment (10 mg/kg) was administered. Previous studies have determined the LD_{50} of PPF in rats to be 22.6 mg/kg, which is significantly higher than the 10 mg/kg used in this study, confirming its safety [38]. Neurological function scores revealed that MCAO/R rats exhibited severe neuronal damage, which was alleviated by PPF treatment (Figure 1B, $P < 0.05$). Cerebral edema was assessed by measuring brain water content, which was elevated in MCAO/R rats but significantly reduced following PPF administration (Figure 1C, $P < 0.05$). TTC staining demonstrated substantial infarct areas in MCAO/R rats, whereas PPF treatment resulted in a notable reduction

Preprint

in infarct size (Figure 1D, $P < 0.05$). HE staining indicated that sham-operated rats had clear and intact tissue structures with dense cell distribution, normal nuclear morphology, and no evidence of tissue hydrolase release. In contrast, MCAO/R rats exhibited loose cell arrangement, neuronal degeneration and necrosis, nuclear shrinkage, obscured nucleoli, and large intercellular voids. PPF treatment significantly attenuated cerebral cortical injury in MCAO/R rats (Figure 1E). Nissl staining revealed severe neuronal loss in MCAO/R rats, which was markedly reduced by PPF treatment (Figure 1F, $P < 0.05$). TUNEL staining showed a significant increase in apoptotic cells in the cerebral cortex of MCAO/R rats, which was decreased by PPF treatment (Figure 1G, $P < 0.05$). Inflammatory and oxidative stress markers, which are central to CI/RI pathophysiology, were elevated in MCAO/R rats. PPF intervention resulted in decreased TNF-α, IL-1β, and MDA, while promoting GSH-Px and SOD activities (Figure 1H-L, $P < 0.05$).

miR-6838-5p Enhances Anti-Inflammatory and Antioxidant Responses in MCAO/R Rats

In the MCAO/R model, the expression of miR-6838-5p was significantly downregulated, as demonstrated by quantitative RT-PCR analysis (Figure 2A, $P < 0.05$). To investigate the functional role of miR-6838-5p in this ischemic injury model, we employed lentiviral vectors to overexpress miR-6838-5p in MCAO/R rats prior to the induction of ischemia-reperfusion. Successful overexpression was confirmed by a substantial increase in miR-6838-5p levels post-injection (Figure 2B, $P < 0.05$). Histological examination revealed that miR-6838-5p overexpression markedly mitigated neuronal damage, as evidenced by reduced neuronal loss and structural preservation in brain tissue sections (Figure 2C, $P < 0.05$). Additionally, rats with elevated miR-6838-5p exhibited a significant decrease in brain water content, indicating reduced cerebral edema (Figure 2D, $P < 0.05$), and a notable reduction in infarct size, assessed through infarct volume measurements (Figure 2E, $P < 0.05$). Further pathological assessment using HE staining demonstrated that miR-6838-5p overexpression led to improved brain tissue morphology, with fewer signs of necrosis and inflammation compared to control groups (Figure 2F). Apoptotic analysis via TUNEL staining revealed a significant decrease in neuronal apoptosis in the miR-6838-5p overexpressing group (Figures 2G and 2H, $P < 0.05$). On a molecular level, overexpression of miR-6838-5p was associated with suppressed inflammatory responses, as indicated by reduced TNF-α and IL-1β (Figures 2I and 2J, $P < 0.05$). Concurrently, markers of oxidative stress were ameliorated; MDA levels were significantly decreased (Figure 2K, $P < 0.05$), while the activities of GSH-Px and SOD were markedly increased (Figures 2L and 2M, $P < 0.05$). Collectively, these results suggest that miR-6838-5p plays a pivotal role in enhancing anti-inflammatory and antioxidant defenses, thereby conferring neuroprotection in MCAO/R-induced ischemic injury.

Inhibition of miR-6838-5p Diminishes the Therapeutic Efficacy of PPF in MCAO/R Rats

Treatment with PPF was found to restore the suppressed expression of miR-6838-5p in MCAO/R rats, as evidenced by increased miR-6838-5p levels post-PPF administration (Figure 3A, $P < 0.05$). To delineate the interaction between PPF and miR-6838-5p, a miR-6838-5p antagonist was administered alongside PPF treatment to effectively inhibit miR-6838-5p expression, which was confirmed by RT-qPCR (Figure 3B, $P < 0.05$). The inhibition of miR-6838-5p significantly abrogated the neuroprotective effects of PPF in MCAO/R rats. Specifically, neuronal injury scores were elevated (Figure 3C, $P < 0.05$), indicating increased neuronal damage. Additionally, brain water content was significantly higher in the miR-6838-5p-inhibited group, suggesting exacerbated cerebral edema (Figure 3D, $P < 0.05$). Infarct size measurements revealed an enlargement of the infarct area upon miR-6838-5p inhibition (Figure 3E, $P < 0.05$). Histopathological analysis using HE staining showed aggravated brain tissue pathology, characterized by increased necrosis and inflammation (Figure 3F). TUNEL assays further confirmed an increase in neuronal apoptosis in the miR-6838-5p-inhibited group (Figures 3G and 3H, $P < 0.05$). At the molecular level, inhibition of miR-6838-5p led to elevated TNF-α and IL-1β (Figures 3I and 3J, $P < 0.05$), as well as increased MDA levels (Figure 3K, $P < 0.05$), indicating heightened oxidative stress. Conversely, the activities of antioxidant enzymes GSH-Px and SOD were significantly suppressed (Figures 3L and 3M, $P < 0.05$). These findings collectively demonstrate

Preprint

that miR-6838-5p is indispensable for the therapeutic efficacy of PPF, as its inhibition negates the anti-inflammatory and antioxidant benefits conferred by PPF treatment in MCAO/R-induced ischemic injury.

miR-6838-5p Regulates AQP11 Expression

We identified potential downstream targets using bioinformatics prediction tools (Figure 4A). AQP11 emerged as a promising candidate target of miR-6838-5p. Dual luciferase reporter assays were conducted to validate this interaction. The results demonstrated that miR-6838-5p mimics significantly inhibited the luciferase activity of the AQP11-WT but had no effect on the AQP11-MUT, confirming a direct binding interaction between miR-6838-5p and the 3' UTR of AQP11 mRNA (Figure 4B, $P < 0.05$). Further validation was performed using RIP assays, which revealed that miR-6838-5p was significantly enriched in complexes containing AQP11, thereby corroborating the direct interaction between the two molecules (Figure 4C, $P < 0.05$). Subsequent analysis of protein expression levels in brain tissues of MCAO/R rats overexpressing miR-6838-5p showed a significant reduction in AQP11 expression (Figure 4D, $P < 0.05$). Importantly, the expression levels of other aquaporin family members, including AQP1, AQP4, and AQP9, remained unchanged, indicating the specificity of miR-6838-5p in targeting AQP11 (Figure 4E, $P < 0.05$). These results collectively establish AQP11 as a direct and specific target of miR-6838-5p, suggesting that the regulatory axis miR-6838-5p/AQP11 plays a crucial role in mediating the anti-inflammatory and antioxidant responses in ischemic injury.

Overexpression of AQP11 Impairs the Therapeutic Effects of PPF in MCAO/R Rats

In the MCAO/R rat model, both AQP11 and AQP4 expression levels were significantly elevated, as determined by RT-qPCR and Western blot analyses (Figures 5A and 5B, $P < 0.05$). PPF treatment effectively reduced the expression of these aquaporins, suggesting a modulatory role of PPF on their expression. To further investigate the specific role of AQP11 in mediating the therapeutic effects of PPF, AQP11 was overexpressed in MCAO/R rats prior to administering PPF, which was confirmed by RT-qPCR and Western blot (Figure 5C, $P < 0.05$). Overexpression of AQP11 in MCAO/R rats undergoing PPF treatment resulted in a significant increase in neuronal injury scores, indicating exacerbated neuronal damage despite PPF administration (Figure 5D, $P < 0.05$). Additionally, brain water content was markedly elevated in the AQP11-overexpressing group (Figure 5E, $P < 0.05$), suggesting aggravated cerebral edema. Infarct size measurements revealed that AQP11 overexpression led to significantly larger infarct areas in PPF-treated MCAO/R rats (Figure 5F, $P < 0.05$). Histopathological analysis using HE staining showed that AQP11 overexpression aggravated brain tissue damage, characterized by increased necrosis and inflammatory cell infiltration (Figure 5G). TUNEL assays confirmed a significant increase in neuronal apoptosis in the AQP11-overexpressing group (Figures 5H and 5I, $P < 0.05$). Elevating AQP11 elevated TNF-α and IL-1β (Figures 5J and 5K, $P < 0.05$), as well as increased MDA levels (Figure 5L, $P < 0.05$). Concurrently, the activities of GSH-Px and SOD were significantly reduced (Figures 5M and 5N, $P < 0.05$). These findings demonstrate that elevating AQP11 undermines the neuroprotective effects of PPF, thereby highlighting the critical role of the miR-6838-5p/AQP11 axis in mediating the therapeutic actions of PPF in MCAO/R-induced ischemic injury.

PPF Alleviates H/R Injury in PC12 Cells via the miR-6838-5p/AQP11 Axis

To translate our in vivo findings to an in vitro context, we utilized a PC12 cell model subjected to H/R injury. In this model, miR-6838-5p expression was markedly decreased, while AQP11 expression was significantly increased, mirroring the in vivo MCAO/R findings (Figures 6A-C, $P < 0.05$). Pretreatment with PPF effectively reversed these expression changes, resulting in elevated miR-6838-5p levels and reduced AQP11 expression (Figures 6A-C, $P < 0.05$), suggesting that PPF modulates the miR-6838-5p/AQP11 axis in vitro. Functional assays further elucidated the protective effects of PPF in PC12 cells subjected to H/R injury. The MTT assay revealed that H/R significantly reduced cell viability (Figure 6D, $P < 0.05$), whereas PPF treatment substantially enhanced cell viability, approaching baseline levels. Flow cytometry analysis demonstrated that H/R induced a significant increase in apoptotic cells (Figure 6E, $P < 0.05$), which was

Preprint

effectively mitigated by PPF treatment, indicating its anti-apoptotic properties. Moreover, oxidative stress markers were assessed to evaluate the antioxidant effects of PPF. H/R resulted in a significant increase in MDA levels and a concomitant decrease in the activities of GSH-Px and SOD in PC12 cells (Figures 6F-H, $P < 0.05$). PPF treatment effectively reversed these alterations by reducing MDA levels and restoring GSH-Px and SOD activities. These in vitro results corroborate the in vivo data, demonstrating that PPF alleviates H/R-induced cellular injury through the modulation of the miR-6838-5p/AQP11 axis, thereby exerting anti-inflammatory and antioxidant effects.

Discussion

CI/RI poses a significant clinical challenge in the treatment of ischemic stroke [39]. Developing therapeutic agents to alleviate CI/RI is a primary focus in the management of cerebral ischemia. Recent studies have highlighted the potential of PPF as a therapeutic agent for CI/RI. However, the downstream molecular mechanisms mediating its protective effects require further elucidation. This study investigated the protective mechanism of PPF in CI/RI, focusing on the miR-6838-5p/AQP11 axis.

Ischemia-reperfusion injury induces a cascade of physiological and pathological changes, including inflammation, oxidative stress, neuronal apoptosis, and structural brain damage [40, 41]. Our study demonstrated that PPF treatment in MCAO/R rats and H/R-injured PC12 cells resulted in decreased neuronal injury scores, reduced brain water content, improved brain histopathology, decreased neuronal apoptosis, and attenuated oxidative stress and inflammatory responses. These findings indicate that PPF effectively promotes the repair of CI/RI and the recovery of neurological function.

MiRNAs are extensively found in eukaryotic organisms and are essential for controlling gene expression in biological processes. [42]. Numerous studies have identified the involvement of miRNAs in CI/RI pathophysiology, including miR-374 [44] and miR-219a-5p [44]. Consequently, miRNAs are considered important therapeutic targets in CI/RI progression. Recently, miR-6838-5p has emerged as a miRNA associated with cardiovascular diseases, implicated in the pathogenesis of cerebral hemorrhage injury [39] and myocardial ischemia-reperfusion injury [46]. Notably, our study observed a downregulation of miR-6838-5p during MCAO/R modeling. Lentiviral overexpression of miR-6838-5p prior to MCAO/R surgery mitigated inflammation and oxidative stress in MCAO/R rats. miR-6838-5p expression was restored in MCAO/R rats following PPF treatment, hinting at a regulatory relationship between PPF and miR-6838-5p Functional rescue experiments confirmed that PPF ameliorates pathological damage in MCAO/R rats by upregulating miR-6838-5p.

miRNAs regulate target gene expression by binding to the 3’ UTR of mRNAs [47]. To shed more light on the involvement of miR-6838-5p in CI/RI, we identified AQP11 as a direct target. AQP11 is an intracellular aquaporin that is expressed in multiple tissues, including the brain [48]. miRNA-mediated regulation of AQP11 safeguards against the disruption of the blood-brain barrier and brain injury after intracerebral hemorrhage [49]. In our study, overexpression of AQP11 in MCAO/R rats exacerbated pathological damages, including increased neuronal injury scores, elevated cerebral water content, aggravated brain histopathology, heightened neuronal apoptosis, and enhanced inflammatory and oxidative stress responses.

Therapeutic interventions often exert their effects through downstream molecular pathways. For instance, sevoflurane modulates CI/RI pathophysiology by targeting homeodomain-interacting protein kinase 1 through upregulation of miR-30c-5p [50], while melatonin targets the miR-26a-5p-neuron restrictive silencer factor pathway to enhance autophagy, control inflammation, and lessen oxidative stress in CI/RI. Our study similarly observed that AQP11 expression increased in MCAO/R rats and was significantly lowered with PPF treatment. These findings imply that PPF's protective effect on CI/RI is mediated by miR-6838's regulation of AQP11. Specifically, PPF enhances miR-6838-5p expression, which in turn downregulates AQP11, leading to reduced pro-inflammatory factors and oxidative stress indicators, thereby mitigating pathological injury in MCAO/R

Preprint

rats. Additionally, PPF attenuates H/R injury in PC12 cells by targeting AQP11 through the upregulation of miR-6838-5p, further supporting the in vivo findings. Furthermore, PPF may influence upstream regulators of miR-6838-5p, thereby providing a broader understanding of its neuroprotective mechanisms. For example, miR-6838-5p has been found to be targeted for adsorption by a circRNA called CircRBM33 in CI/RI [24]. In addition to circRNAs, lncRNAs may also be upstream targets of PPF regulation. In cancer, lncRNA CERS6-AS1 and lncRNA SH3BP5-AS1 are shown to target adsorption of miR-6838-5p [51, 52]. Therefore, it is necessary to further explore the PPF-influenced circRNAs and lncRNAs by sequencing technology in future studies to further confirm the upstream genes of miR-6838-5p. While our study focused on the downstream effects involving miR-6838-5p and AQP11, it is plausible that PPF interacts with key transcription factors such as NF-κB and Nrf2, or epigenetic regulators like histone modifying enzymes, to indirectly regulate the expression of miR-6838-5p. Identifying these upstream regulators remains a crucial area for future research, which could be pursued through techniques such as chromatin immunoprecipitation and RNA sequencing to map the regulatory networks influenced by PPF.

Despite confirming the protective effects and underlying mechanisms of PPF against CI/RI, this study has certain limitations. Firstly, upstream regulatory molecules of miR-6838-5p were not explored, which could provide a more comprehensive understanding of the protective mechanisms of PPF in CI/RI. Secondly, potential anti-endoplasmic reticulum stress and other protective effects of PPF were not investigated, which could further elucidate the pharmacological profile of PPF. Moreover, the clinical significance of PPF in CI/RI remains to be evaluated. Currently, the application of PPF for CI/RI treatment is limited to in vitro and animal studies, and its clinical use faces significant challenges. The molecular mechanisms by which PPF ameliorates CI/RI are not fully defined, and the appropriate dosing and toxicity of PPF in humans require further investigation. Notably, PPF infusion syndrome (PRIS), a potentially fatal condition, underscores the need to explore PPF toxicity [53]. Future research should focus on delineating the molecular mechanisms of PPF in CI/RI, assessing its toxicity, and identifying agents that can mitigate PRIS. Additionally, combination therapies involving PPF and other drugs may offer a promising approach for effective CI/RI treatment. Additionally, future studies should explore the role of PPF in other models of neuroprotection and assess the combined effects of multiple therapeutic strategies to enhance treatment efficacy. Combination therapies involving PPF and other drugs may offer a promising approach for effective CI/RI treatment.

Moreover, the potential risks associated with targeting miR-6838-5p must be carefully considered, given that miRNAs are widely expressed across multiple tissues. Targeting miR-6838-5p may have unintended off-target effects, potentially affecting the function of other organs such as the heart, liver, and kidneys. Future studies should employ tissue-specific knockdown or overexpression models to evaluate the safety and specificity of miR-6838-5p modulation. Additionally, exploring delivery methods that ensure brain-specific targeting, such as brain-targeted vectors or localized administration, could minimize systemic side effects and enhance therapeutic efficacy. Understanding these aspects is crucial for the safe and effective clinical translation of therapies targeting the miR-6838-5p/AQP11 axis.

This study aligns with previous research on the neuroprotective mechanisms of other anesthetic agents, such as sevoflurane and melatonin, which also modulate specific miRNA axes to exert their protective effects. However, our study is the first to elucidate the role of the miR-6838-5p/AQP11 axis in PPF-mediated neuroprotection in CI/RI, thereby highlighting a novel therapeutic pathway that could be targeted in future interventions. This novel insight provides a solid foundation for therapeutic strategies targeting the miR-6838-5p/AQP11 axis, potentially enhancing the clinical management of ischemic stroke and reducing the associated neurological damage.

Moreover, the study's comprehensive experimental framework, which includes both in vivo and in vitro models, strengthens the validity of the results and supports the translational potential of targeting the miR-6838-5p/AQP11 axis. Future studies should strive to confirm these findings in clinical trials and assess the

Preprint

broader implications of targeting this axis in other tissues, taking into account the widespread expression of miRNAs and possible off-target effects. Additionally, investigating the long-term effects of miR-6838-5p modulation and PPF treatment on neuronal function and behavioral outcomes will be essential for understanding the sustained impact and safety of such therapeutic interventions.

Conclusion

PPF attenuates oxidative stress injury and inflammation in MCAO/R rats and H/R-injured PC12 cells by targeting AQP11 through the upregulation of miR-6838-5p. This study is the first to elucidate the role of the PPF/miR-6838-5p/AQP11 axis in cerebral ischemia-reperfusion injury, providing novel targets for drug development and therapeutic strategies for CI/RI following ischemic stroke. Future studies should validate these findings through clinical trials, employing multicenter approaches to enhance the generalizability and reproducibility of the results. Additionally, randomized controlled trials should compare the efficacy of PPF with existing treatments, optimize dosing regimens, and assess the safety profile of PPF in human populations. Evaluating the impact of PPF on the clinical prognosis of patients with CI/RI is also essential to translate these preclinical findings into effective clinical interventions. Furthermore, exploring the potential synergistic effects of PPF with other therapeutic agents targeting different molecular pathways may offer more comprehensive neuroprotection and improved clinical outcomes.

Acknowledgments

Not applicable.

Funding

This study was supported by the Shandong Province Traditional Chinese Medicine Science and Technology Project (2021Z009).

Competing interests

The authors have no conflicts of interest to declare.

Availability of data and materials

The datasets used and/or analyzed during the present study are available from the corresponding author on reasonable request.

Ethics statement

The animal experiment research protocol was approved by the Ethics Committee of our Hospital (SDTHEC) and performed in accordance with the “Guidelines for the care and use of experimental animals.”

References

1. Benjamin EJ, Blaha MJ, Chiuve SE, Cushman M, Das SR, Deo R, et al. Heart Disease and Stroke Statistics-2017 Update: A Report From the American Heart Association. Circulation. 2017;135(10):e146-e603.
2. Lo WL, Mao YR, Li L, Lin AH, Zhao JL, Chen L, et al. Prospective clinical study of rehabilitation interventions with multisensory interactive training in patients with cerebral infarction: study protocol for a randomised controlled trial. Trials. 2017;18(1):173.
3. Feske, S.K., Ischemic Stroke. Am J Med, 2021. 134(12): p. 1457-1464.
4. Obadia N, Lessa MA, Daliry A, Silvares RR, Gomes F, Tibiriçá E, et al. Cerebral microvascular dysfunction in metabolic syndrome is exacerbated by ischemia-reperfusion injury. BMC Neurosci.

Preprint

2017;18(1):67.
5. Xue X, Wang H, Su J. Inhibition of MiR-122 Decreases Cerebral Ischemia-reperfusion Injury by Upregulating DJ-1-Phosphatase and Tensin Homologue Deleted on Chromosome 10 (PTEN)/Phosphonosinol-3 Kinase (PI3K)/AKT. Med Sci Monit. 2020;26:e915825.
6. Zhou X, Wang Z, Xu B, Ji N, Meng P, Gu L, et al. Long non-coding RNA NORAD protects against cerebral ischemia/reperfusion injury induced brain damage, cell apoptosis, oxidative stress and inflammation by regulating miR-30a-5p/YWHAG. Bioengineered. 2021;12(2):9174-88.
7. Wu MY, Yiang GT, Liao WT, Tsai AP, Cheng YL, Cheng PW, et al. Current Mechanistic Concepts in Ischemia and Reperfusion Injury. Cell Physiol Biochem. 2018;46(4):1650-67.
8. Herpich, F. and F. Rincon, Management of Acute Ischemic Stroke. Crit Care Med, 2020. 48(11): p. 1654-1663.
9. Amani H, Mostafavi E, Alebouyeh MR, Arzaghi H, Akbarzadeh A, Pazoki-Toroudi H, et al. Would Colloidal Gold Nanocarriers Present An Effective Diagnosis Or Treatment For Ischemic Stroke? Int J Nanomedicine. 2019;14:8013-31.
10. Zhu, X.N., et al., Propofol exerts anti-anhedonia effects via inhibiting the dopamine transporter. Neuron, 2023. 111(10): p. 1626-1636 e6.
11. Guo, X.N. and X. Ma, The Effects of Propofol on Autophagy. DNA Cell Biol, 2020. 39(2): p. 197-209.
12. Fan W, Zhu X, Wu L, Wu Z, Li D, Huang F, et al. Propofol: an anesthetic possessing neuroprotective effects. Eur Rev Med Pharmacol Sci. 2015;19(8):1520-9.
13. Tao W, Zhang X, Ding J, Yu S, Ge P, Han J, et al. The effect of propofol on hypoxia- and TNF-α-mediated BDNF/TrkB pathway dysregulation in primary rat hippocampal neurons. CNS Neurosci Ther. 2022;28(5):761-74.
14. Engelhard K, Werner C, Eberspächer E, Pape M, Stegemann U, Kellermann K, et al. Influence of propofol on neuronal damage and apoptotic factors after incomplete cerebral ischemia and reperfusion in rats: a long-term observation. Anesthesiology. 2004;101(4):912-7.
15. Huang L, Ding L, Yu S, Huang X, Ren Q. Propofol postconditioning alleviates diabetic myocardial ischemia-reperfusion injury via the miR-200c-3p/AdipoR2/STAT3 signaling pathway. Mol Med Rep. 2022;25(4).
16. Zhou R, Yang Z, Tang X, Tan Y, Wu X, Liu F. Propofol protects against focal cerebral ischemia via inhibition of microglia-mediated proinflammatory cytokines in a rat model of experimental stroke. PLoS One. 2013;8(12):e82729.
17. Gao X, Mi Y, Guo N, Luan J, Xu H, Hu Z, et al. The mechanism of propofol in cancer development: An updated review. Asia Pac J Clin Oncol. 2020;16(2):e3-e11.
18. Feng L, Sun ZG, Liu QW, Ma T, Xu ZP, Feng ZG, et al. Propofol inhibits the expression of Abelson nonreceptor tyrosine kinase without affecting learning or memory function in neonatal rats. Brain Behav. 2020;10(11):e01810.
19. Romuk EB, Szczurek W, Nowak PG, Hudziec E, Chwalińska E, Birkner E. Effects of Propofol on the Liver Oxidative-Antioxidant Balance in a Rat Model of Parkinson's Disease. Adv Clin Exp Med. 2016;25(5):815-20.
20. Yu W, Gao D, Jin W, Liu S, Qi S. Propofol Prevents Oxidative Stress by Decreasing the Ischemic Accumulation of Succinate in Focal Cerebral Ischemia-Reperfusion Injury. Neurochem Res. 2018;43(2):420-9.
21. Jia L, Wang F, Gu X, Weng Y, Sheng M, Wang G, et al. Propofol postconditioning attenuates hippocampus ischemia-reperfusion injury via modulating JAK2/STAT3 pathway in rats after autogenous orthotropic liver transplantation. Brain Res. 2017;1657:202-7.
22. Chen Y, Li Z. Protective Effects of Propofol on Rats with Cerebral Ischemia-Reperfusion Injury Via the

Preprint

PI3K/Akt Pathway. J Mol Neurosci. 2021;71(4):810-20.
23. Hausburg MA, Banton KL, Roman PE, Salgado F, Baek P, Waxman MJ, et al. Effects of propofol on ischemia-reperfusion and traumatic brain injury. J Crit Care. 2020;56:281-7.
24. Zhang, Y., et al., CircRBM33 induces endothelial dysfunction by targeting the miR-6838-5p/PDCD4 axis affecting blood-brain barrier in mice with cerebral ischemia-reperfusion injury. Clin Hemorheol Microcirc, 2023. 85(4): p. 355-370.
25. Morishita, Y., et al., Disruption of aquaporin-11 produces polycystic kidneys following vacuolization of the proximal tubule. Mol Cell Biol, 2005. 25(17): p. 7770-9.
26. Gorelick, D.A., et al., Aquaporin-11: a channel protein lacking apparent transport function expressed in brain. BMC Biochem, 2006. 7: p. 14.
27. Zuo ML, Wang AP, Song GL, Yang ZB. miR-652 protects rats from cerebral ischemia/reperfusion oxidative stress injury by directly targeting NOX2. Biomed Pharmacother. 2020;124:109860.
28. Sun B, Ou H, Ren F, Guan Y, Huan Y, Cai H. Propofol Protects against Cerebral Ischemia/Reperfusion Injury by Down-Regulating Long Noncoding RNA SNHG14. ACS Chem Neurosci. 2021;12(16):3002-14.
29. Liang, C., et al., Propofol attenuates cerebral ischemia/reperfusion injury partially using heme oxygenase-1. J Neurosurg Anesthesiol, 2013. 25(3): p. 311-6.
30. Sun, B., et al., Propofol Protects against Cerebral Ischemia/Reperfusion Injury by Down-Regulating Long Noncoding RNA SNHG14. ACS Chem Neurosci, 2021. 12(16): p. 3002-3014.
31. Lu Y, Han Y, He J, Zhou B, Fang P, Li X. LncRNA FOXD3-AS1 knockdown protects against cerebral ischemia/reperfusion injury via miR-765/BCL2L13 axis. Biomed Pharmacother. 2020;132:110778.
32. Wang C, Hu F. Long noncoding RNA SOX2OT silencing alleviates cerebral ischemia-reperfusion injury via miR-135a-5p-mediated NR3C2 inhibition. Brain Res Bull. 2021;173:193-202.
33. Yang B, Zang LE, Cui JW, Zhang MY, Ma X, Wei LL. Melatonin Plays a Protective Role by Regulating miR-26a-5p-NRSF and JAK2-STAT3 Pathway to Improve Autophagy, Inflammation and Oxidative Stress of Cerebral Ischemia-Reperfusion Injury. Drug Des Devel Ther. 2020;14:3177-88.
34. Hu Y, Ye C, Cheng S, Chen J. Propofol Downregulates lncRNA MALAT1 to Alleviate Cerebral Ischemia-Reperfusion Injury. Inflammation. 2021;44(6):2580-91.
35. Chen C, Chang X, Zhang S, Zhao Q, Lei C. CircRNA CTNNB1 (circCTNNB1) ameliorates cerebral ischemia/reperfusion injury by sponging miR-96-5p to up-regulate scavenger receptor class B type 1 (SRB1) expression. Bioengineered. 2022;13(4):10258-73.
36. Li J, He W, Wang Y, Zhao J, Zhao X. miR-103a-3p alleviates oxidative stress, apoptosis, and immune disorder in oxygen-glucose deprivation-treated BV2 microglial cells and rats with cerebral ischemia-reperfusion injury by targeting high mobility group box 1. Ann Transl Med. 2020;8(20):1296.
37. Kuai F, Zhou L, Zhou J, Sun X, Dong W. Long non-coding RNA THRIL inhibits miRNA-24-3p to upregulate neuropilin-1 to aggravate cerebral ischemia-reperfusion injury through regulating the nuclear factor κB p65 signaling. Aging (Albany NY). 2021;13(6):9071-84.
38. Wang B, Chen S, Yang J, Yang L, Liu J, Zhang W. ET-26 hydrochloride (ET-26 HCl) has similar hemodynamic stability to that of etomidate in normal and uncontrolled hemorrhagic shock (UHS) rats. PLoS One. 2017;12(8):e0183439.
39. Liu H, Wu X, Luo J, Zhao L, Li X, Guo H, et al. Adiponectin peptide alleviates oxidative stress and NLRP3 inflammasome activation after cerebral ischemia-reperfusion injury by regulating AMPK/GSK-3β. Exp Neurol. 2020;329:113302.
40. Liang Q, Yang J, He J, Chen X, Zhang H, Jia M, et al. Stigmasterol alleviates cerebral ischemia/reperfusion injury by attenuating inflammation and improving antioxidant defenses in rats. Biosci Rep. 2020;40(4).

Preprint

41. Leech T, Chattipakorn N, Chattipakorn SC. The beneficial roles of metformin on the brain with cerebral ischaemia/reperfusion injury. Pharmacol Res. 2019;146:104261.
42. Lu TX, Rothenberg ME. MicroRNA. J Allergy Clin Immunol. 2018;141(4):1202-7.
43. Xing F, Liu Y, Dong R, Cheng Y. miR-374 improves cerebral ischemia reperfusion injury by targeting Wnt5a. Exp Anim. 2021;70(1):126-36.
44. Lu MY, Wu JR, Liang RB, Wang YP, Zhu YC, Ma ZT, et al. Upregulation of miR-219a-5p Decreases Cerebral Ischemia/Reperfusion Injury In Vitro by Targeting Pde4d. J Stroke Cerebrovasc Dis. 2020;29(6):104801.
45. Jiang F, Liu X, Wang X, Hu J, Chang S, Cui X. LncRNA FGD5-AS1 accelerates intracerebral hemorrhage injury in mice by adsorbing miR-6838-5p to target VEGFA. Brain Res. 2022;1776:147751.
46. Zhang G, Ding L, Sun G, Liu Z, Ou W, Wang B, et al. LncRNA AZIN1-AS1 ameliorates myocardial ischemia-reperfusion injury by targeting miR-6838-5p/WNT3A axis to activate Wnt-β/catenin signaling pathway. In Vitro Cell Dev Biol Anim. 2022;58(1):54-68.
47. Bartel DP. MicroRNAs: genomics, biogenesis, mechanism, and function. Cell. 2004;116(2):281-97.
48. Koike S, Tanaka Y, Matsuzaki T, Morishita Y, Ishibashi K. Aquaporin-11 (AQP11) Expression in the Mouse Brain. Int J Mol Sci. 2016;17(6).
49. Xi T, Jin F, Zhu Y, Wang J, Tang L, Wang Y, et al. miR-27a-3p protects against blood-brain barrier disruption and brain injury after intracerebral hemorrhage by targeting endothelial aquaporin-11. J Biol Chem. 2018;293(52):20041-50.
50. Su G, Qu Y, Li G, Deng M. Sevoflurane protects against cerebral ischemia/reperfusion injury via microrna-30c-5p modulating homeodomain-interacting protein kinase 1. Bioengineered. 2021;12(2):11858-71.
51. Yan, K., et al., LncRNA CERS6-AS1, sponging miR-6838-5p, promotes proliferation and invasion in cervical carcinoma cells by upregulating FOXP2. Histol Histopathol, 2023. 38(7): p. 823-835.
52. Zhao, X., et al., LncRNA SH3BP5-AS1 promotes hepatocellular carcinoma progression by sponging miR-6838-5p and activation of PTPN4. Aging (Albany NY), 2024. 16(10): p. 8511-8523.
53. Krajčová A, Waldauf P, Anděl M, Duška F. Propofol infusion syndrome: a structured review of experimental studies and 153 published case reports. Crit Care. 2015;19:398.

Preprint

Figure and Table legends

Table 1 Primers used in PCR
Note: miR-6838-5p, microRNA-6838-5p; AQP11, aquaporin11.

Figure 1 PPF attenuates oxidative stress injury in MCAO/R rats.
Chemical structure diagram of PPF (A), Effects of PPF on the neurological function (B), cerebral edema (C), infarction area (D), cerebral cortex histopathology (E), morphology of cerebral cortical neurons (F), apoptosis of rat cerebral cortex (G), inflammatory indicators (H-I), and oxidative stress indexes (J-L). n = 6; * $P < 0.05$.

Figure 2 miR-6838-5p inhibits inflammation and oxidative stress in MCAO/R rats.
MCAO/R-induced change in miR-6838-5p expression in rats (A); Effects of miR-6838-5p lentivirus on miR-6838-5p expression in rat brain tissue (B), neurological function (C), cerebral edema (D), infarction area (E), cerebral cortex histopathology (F), morphology of cerebral cortical neurons (G), apoptosis of rat cerebral cortex (H), inflammatory indicators (I-J), and oxidative stress indexes (K-M). n = 6; * $P < 0.05$.

Figure 3 Inhibiting miR-6838-5p reverses PPF treatment efficacy in MCAO/R rats.
Effects of PPF on miR-6838-5p expression in rat brain tissue (A); Effect of combined miR-6838-5p antagonist + PPF on miR-6838-5p expression in rat brain tissue (B), neurological function (C), cerebral edema (D), infarction area (E), cerebral cortex histopathology (F), morphology of cerebral cortical neurons (G), apoptosis of rat cerebral cortex (H), inflammatory indicators (I-J), and oxidative stress indexes (K-M). n = 6; * $P < 0.05$.

Figure 4 miR-6838-5p targets AQP11.
Binding site of miR-6838-5p to AQP11 (A), confirmation of the binding relationship between miR-6838-5p and AQP11 (B-C), AQP1/AQP4/AQP9/AQP11 expression in rat brain tissue overexpressing miR-6838-5p (D-E). * $P < 0.05$.

Figure 5 Overexpression of AQP11 reduces the therapeutic effect of PPF on MCAO/R rats.
MCAO/R-induced change in AQP11 and AQP4 expression in rat brain tissue and effect of PPF on AQP11 and AQP4 expression in MCAO/R rats (A-B), Effect of combined lV-AQP11 + PPF on AQP11 expression in rat brain tissue (C), neurological function (D), cerebral edema (E), infarction area (F), cerebral cortex histopathology (G), morphology of cerebral cortical neurons (H), apoptosis of rat cerebral cortex (I), inflammatory indicators (J-K), and oxidative stress indexes (L-N). n = 6; * $P < 0.05$.

Figure 6 PPF attenuates H/R injury in PC12 cells by targeting AQP11 by upregulating miR-6838-5p.
Effect of H/R and PPF on miR-6838-5p and AQP11 expression in cells (A-C), viability (D), apoptosis (E), and oxidative stress indicators (F-H). n = 6, * $P < 0.05$.

Preprint

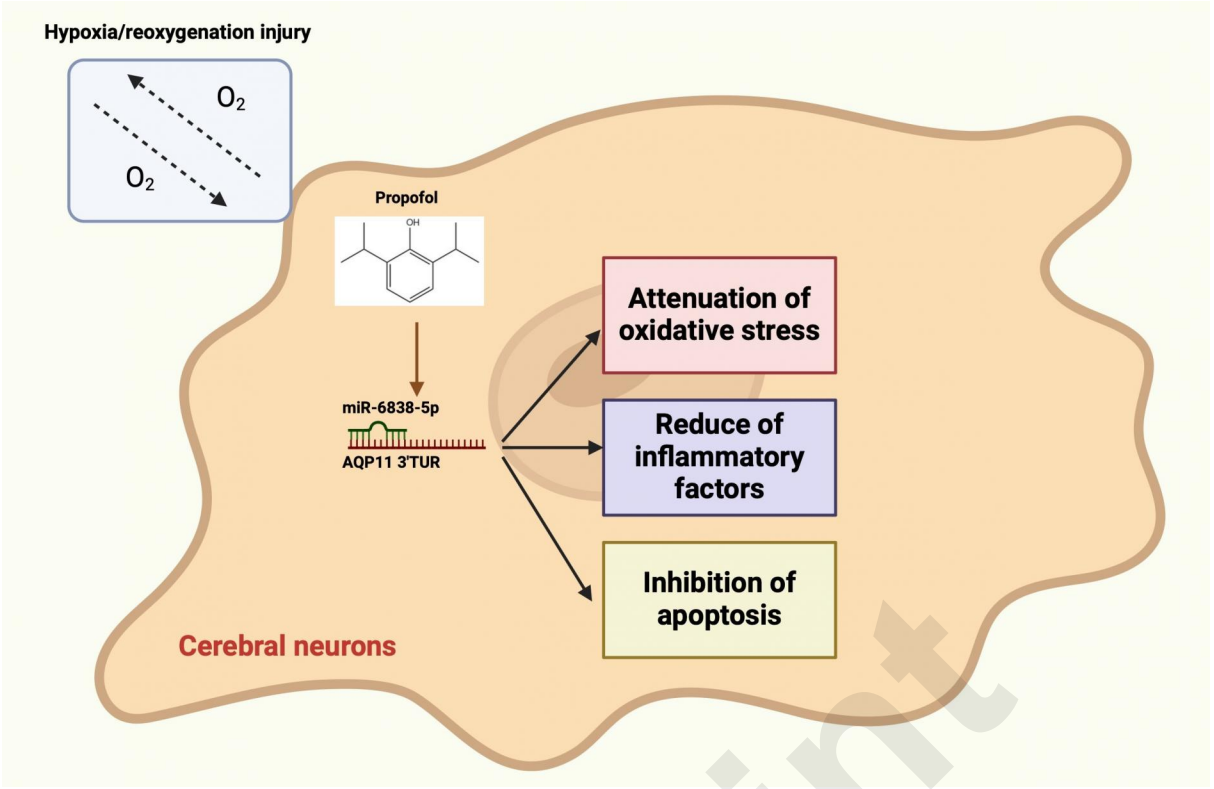
Hypoxia/reoxygenation injury
O_2
O_2
Propofol
OH
miR-6838-5p
AQP11 3'TUR
Attenuation of oxidative stress
Reduce of inflammatory factors
Inhibition of apoptosis
Cerebral neurons

Preprint

Table 1 Primers used in PCR

Genes	Sequence (5′→3′)
miR-6838-5p	F:GCACTCCTGGATGCCAATCT
	R:CTCTACAGCTATATTGCCAGCCAC
AQP11	F:GCCTTCGTCCTGGAGTTTCT
	R:GCACCAAGGAAAAGAAGTAGAT
U6	F:CTCGCTTCGGCAGCACA
	R:AACGCTTCACGAATTTGCGT
β-actin	F:GGAGATTACTGCCCTGGCTCCTAGC
	R:GGCCGGACTCATCGTACTCCTGCTT

Note: miR-6838-5p, microRNA-6838-5p; AQP11, aquaporin11.

Preprint

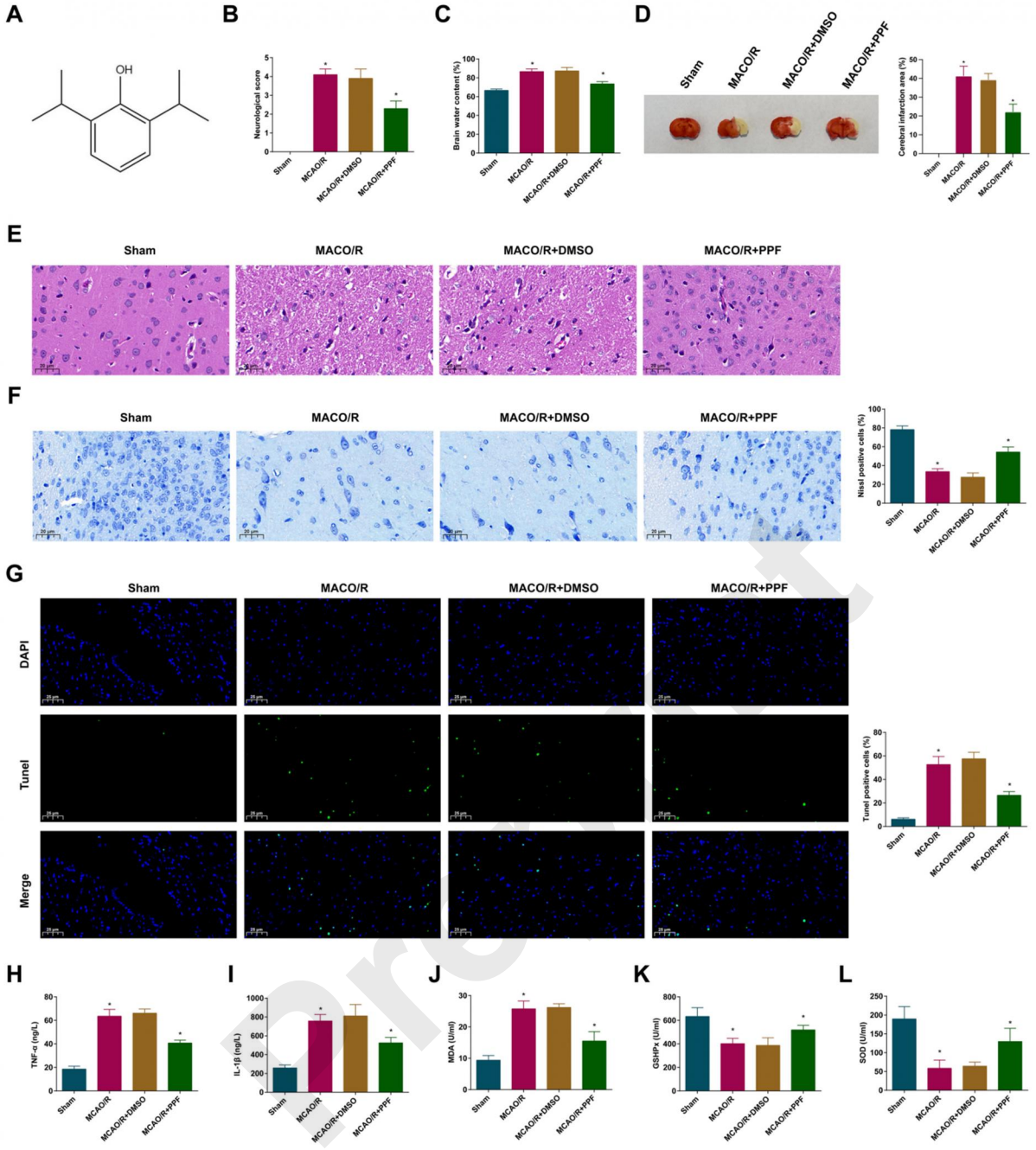
A
OH
B
Neurological score
Sham
MCAO/R
MCAO/R+DMSO
MCAO/R+PPF
C
Brain water content (%)
D
Cerebral infarction area (%)
E
F
Nissl positive cells (%)
G
DAPI
Tunel
Merge
Tunel positive cells (%)
H
TNF-α (ng/L)
I
IL-1β (ng/L)
J
MDA (U/ml)
K
GSHPx (U/ml)
L
SOD (U/ml)

Preprint

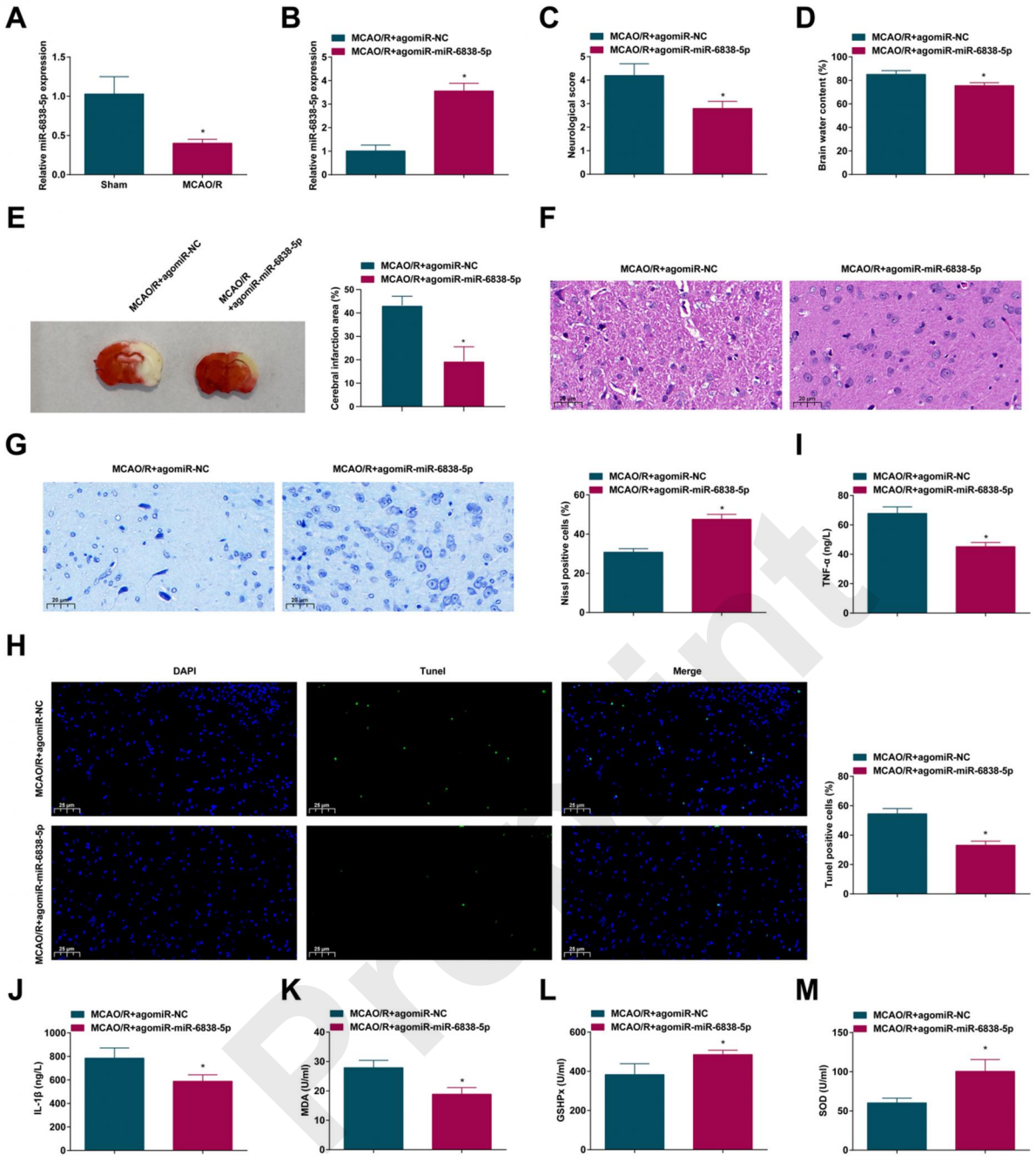
A
Relative miR-6838-5p expression
Sham
MCAO/R
B
MCAO/R+agomiR-NC
MCAO/R+agomiR-miR-6838-5p
Relative miR-6838-5p expression
C
Neurological score
D
Brain water content (%)
E
MCAO/R+agomiR-NC
MCAO/R +agomiR-miR-6838-5p
Cerebral infarction area (%)
F
G
Nissl positive cells (%)
I
TNF-α (ng/L)
H
DAPI
Tunel
Merge
Tunel positive cells (%)
J
IL-1β (ng/L)
K
MDA (U/ml)
L
GSHPx (U/ml)
M
SOD (U/ml)

Preprint

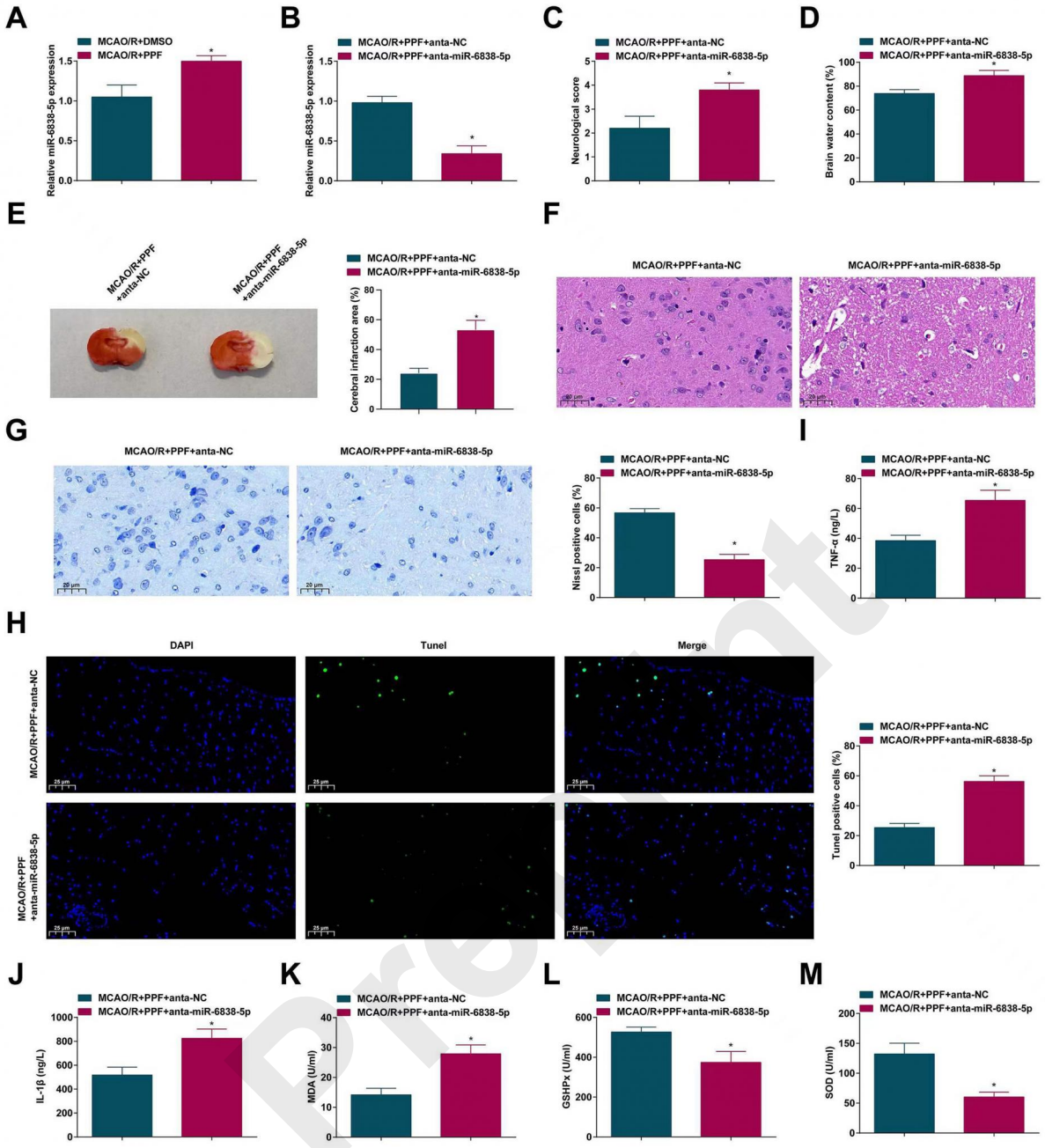
A
MCAO/R+DMSO
MCAO/R+PPF
Relative miR-6838-5p expression
B
MCAO/R+PPF+anta-NC
MCAO/R+PPF+anta-miR-6838-5p
Relative miR-6838-5p expression
C
Neurological score
D
Brain water content (%)
E
MCAO/R+PPF +anta-NC
MCAO/R+PPF +anta-miR-6838-5p
Cerebral infarction area (%)
F
G
Nissl positive cells (%)
I
TNF-α (ng/L)
H
DAPI
Tunel
Merge
Tunel positive cells (%)
J
IL-1β (ng/L)
K
MDA (U/ml)
L
GSHPx (U/ml)
M
SOD (U/ml)

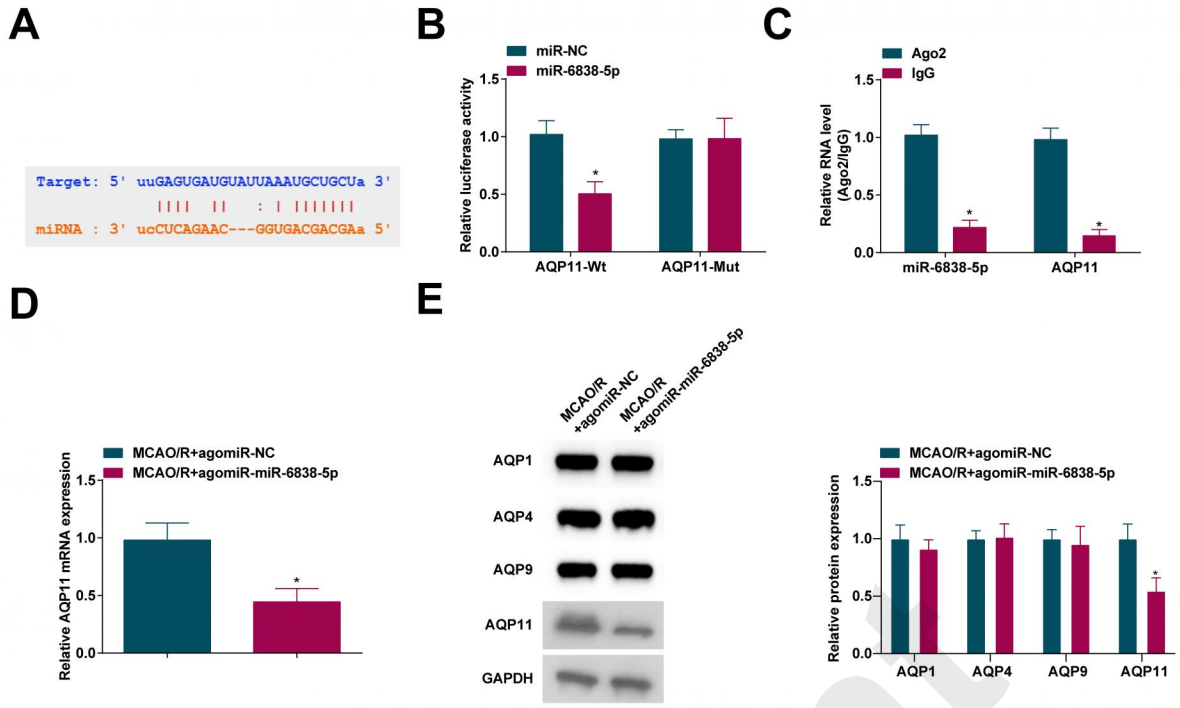
A
Target: 5' uuGAGUGAUGUAUUAAAUGCUGCUa 3'
miRNA : 3' ucCUCAGAAC---GGUGACGACGAa 5'
B
miR-NC
miR-6838-5p
Relative luciferase activity
AQP11-Wt
AQP11-Mut
C
Ago2
IgG
Relative RNA level (Ago2/IgG)
miR-6838-5p
AQP11
D
MCAO/R+agomiR-NC
MCAO/R+agomiR-miR-6838-5p
Relative AQP11 mRNA expression
E
MCAO/R +agomiR-NC
MCAO/R +agomiR-miR-6838-5p
AQP1
AQP4
AQP9
AQP11
GAPDH
MCAO/R+agomiR-NC
MCAO/R+agomiR-miR-6838-5p
Relative protein expression
AQP1
AQP4
AQP9
AQP11

Preprint

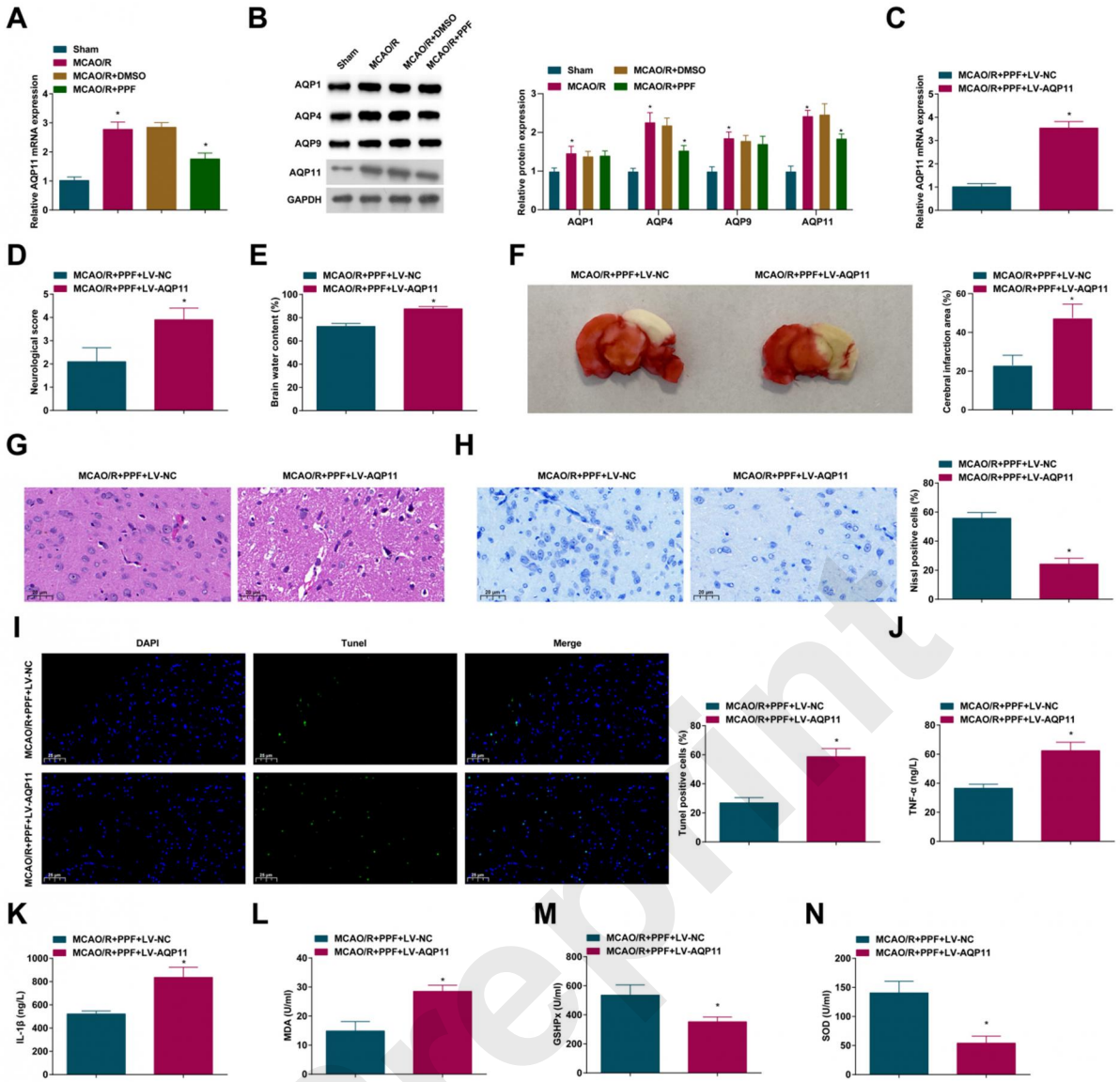
A
Sham
MCAO/R
MCAO/R+DMSO
MCAO/R+PPF
Relative AQP11 mRNA expression
B
Sham
MCAO/R
MCAO/R+DMSO
MCAO/R+PPF
AQP1
AQP4
AQP9
AQP11
GAPDH
Relative protein expression
C
MCAO/R+PPF+LV-NC
MCAO/R+PPF+LV-AQP11
Relative AQP11 mRNA expression
D
Neurological score
E
Brain water content (%)
F
Cerebral infarction area (%)
G
H
Nissl positive cells (%)
I
DAPI
Tunel
Merge
Tunel positive cells (%)
J
TNF-α (ng/L)
K
IL-1β (ng/L)
L
MDA (U/ml)
M
GSHPx (U/ml)
N
SOD (U/ml)

Preprint

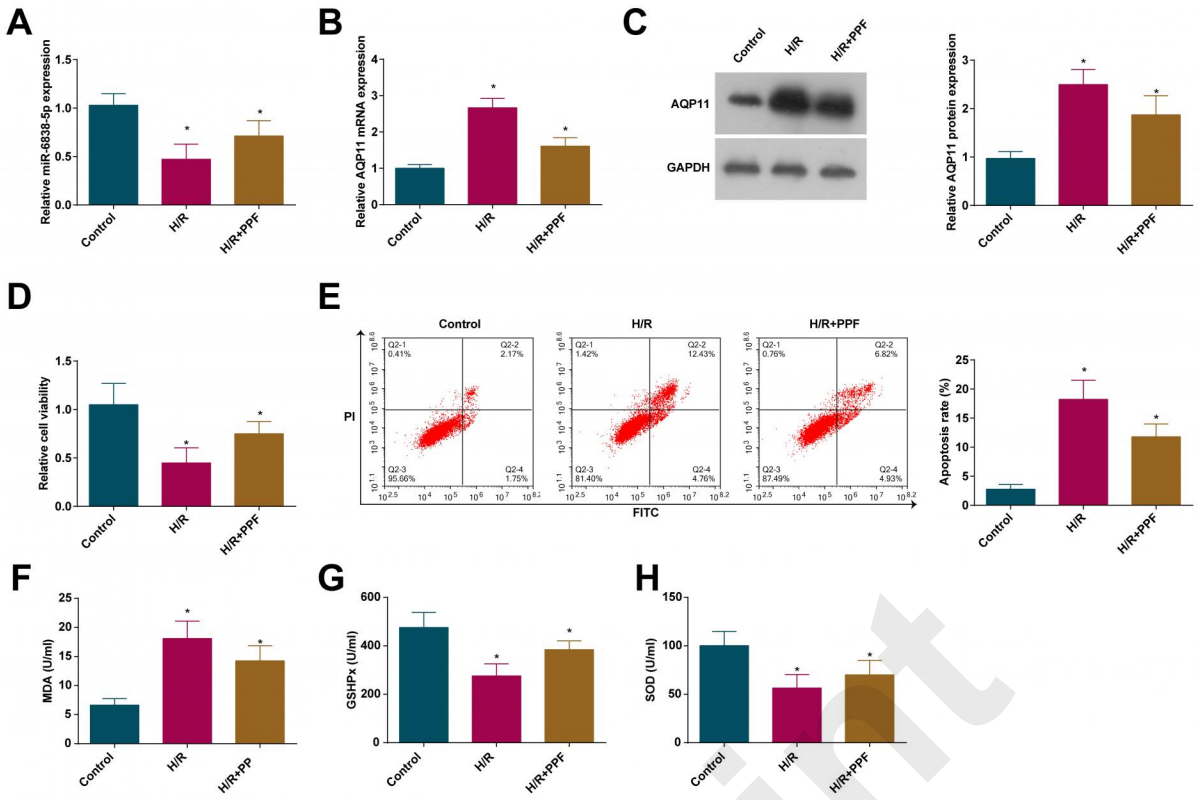
A
Relative miR-6838-5p expression
1.5
1.0
0.5
0.0
Control
H/R
H/R+PPF
B
Relative AQP11 mRNA expression
4
3
2
1
0
Control
H/R
H/R+PPF
C
Control
H/R
H/R+PPF
AQP11
GAPDH
Relative AQP11 protein expression
3
2
1
0
Control
H/R
H/R+PPF
D
Relative cell viability
1.5
1.0
0.5
0.0
Control
H/R
H/R+PPF
E
Control
H/R
H/R+PPF
PI
FITC
Q2-1
0.41%
Q2-2
2.17%
Q2-3
95.66%
Q2-4
1.75%
Q2-1
1.42%
Q2-2
12.43%
Q2-3
81.40%
Q2-4
4.76%
Q2-1
0.76%
Q2-2
6.82%
Q2-3
87.49%
Q2-4
4.93%
Apoptosis rate (%)
25
20
15
10
5
0
Control
H/R
H/R+PPF
F
MDA (U/ml)
25
20
15
10
5
0
Control
H/R
H/R+PP
G
GSHPx (U/ml)
600
400
200
0
Control
H/R
H/R+PPF
H
SOD (U/ml)
150
100
50
0
Control
H/R
H/R+PPF

Preprint